29th EPS Conference on Plasma Phys. and Contr. Fusion Montreux, 17-21 June 2002 ECA Vol. **26B**, P-1.077 (2002)

Transport Analysis of ECH Overlapped NBI Plasmas in LHD

H.Funaba, T.Shimozuma, S.Kubo, H.Idei, Y.Yoshimura, T.Notake [1], K.Narihara, K.Ida, Y.Nagayama, S.Inagaki, Y.Takeiri, M.Osakabe, K.Tanaka, B.J.Peterson, K.Y.Watanabe, S.Murakami, M.Yokoyama, K.Kawahata, N.Ohyabu and the LHD Experimental Group

National Institute for Fusion Science, Toki, Gifu 509-5292, Japan
[1]*Nagoya Univ., Grad. School of Energy Engineering and Science, Nagoya 464-8601, Japan*

1. Introduction

The electron temperature, T_e, profile with a high central T_e and a steep gradient, ∇T_e, was observed on the Large Helical Device (LHD) [1] in both ECH plasmas and low density NBI plasmas with overlapping of the strongly focused ECH [2]. Local transport analysis is carried out in order to clarify whether any transport improvement, such as the electron thermal transport barrier which is observed in the Compact Helical System (CHS) [3], appeared or not in LHD associated with the high central T_e.

The electron thermal conductivities in NBI with ECH plasmas of various densities are evaluated and they are compared with the results of the neoclassical calculation with the radial electric field, E_r. Moreover, some transport simulations of the temporal development of T_e are carried out to evaluate the electron thermal transport at the central region.

2. Transport analysis of ECH overlapped NBI plasmas

In the plasmas heated by NBI and ECH, the high $T_e(0)$ and the steep ∇T_e appeared when the absorbed power of ECH, P_{ECH}, exceeded a certain threshold power or the electron density, n_e, was lower than a threshold density. Figure 1 (a) shows four profiles of T_e, which were measured by the YAG Thomson scattering system [4]. Three of them are in the cases of NBI with ECH heated plasmas with different n_e ($\bullet : \overline{n}_e = 0.15 \times 10^{19}\,\mathrm{m}^{-3}$, $\triangle : 0.24 \times 10^{19}\,\mathrm{m}^{-3}$ and $\diamond : 1.7 \times 10^{19}\,\mathrm{m}^{-3}$) and the other symbol (+) represents T_e in a NBI-only plasma. Here, $\rho = (\Phi/\Phi_a)^{1/2}$ ($\Phi :$ the toroidal magnetic flux) is the normalized average minor radius and $\rho < 0$ denotes the inside of the magnetic axis position, R_{ax}. These plasmas are produced under the conditions of $R_{ax} = 3.75\,\mathrm{m}$ (the standard magnetic configuration) and the magnetic field strength $B = 1.52\,\mathrm{T}$. The spatial profile of E_r can be measured in the $R_{ax} = 3.75\,\mathrm{m}$ case by the charge exchange spectroscopy (CXS) [5, 6] of NeX with the neon gas puffing. $B = 1.52\,\mathrm{T}$ is adjusted to the central heating condition of the 2nd harmonic ECH. In the lowest n_e case ($\bullet$), the T_e profile has $T_e(0) \geq 8\,\mathrm{keV}$. The steep ∇T_e appears in the low density cases ($\bullet$, $\triangle$) at the $\rho < 0.2$ region. However, such ∇T_e can't be seen in the high density case ($\diamond$).

The experimental thermal diffusivities, χ_e for electrons and χ_i for ions, are evaluated by the local transport analysis using an one-dimensional transport code, PROCTR [7].

This code reads the magnetic flux surface data and the spatial profiles of T_e, n_e, the ion temperature, T_i, the absorbed power of ECH, P_{ECH}, the deposition power of NBI to electrons and ions, P^e_{NBI} and P^i_{NBI}, the radiation power, P_{rad}, and so on. $P^e_{NBI}(\rho)$ and $P^i_{NBI}(\rho)$ are given by the calculation results from a three-dimensional Monte Carlo simulation code [8]. $P_{ECH}(\rho)$ is calculated by the ray-tracing method. Its profile depends on the focal point and the R_{ax} shift by β.

χ_e^{exp} in the NBI-only case is about $12\,\mathrm{m^2/s}$ at the center and it gradually decreases towards the edge as shown in Fig.1(b). The magnitude of χ_e^{exp} in the high density NBI with ECH plasma becomes large at the central region because of the increase in the deposition power to electrons. On the other hand, the central χ_e^{exp} was reduced in the case of the low density NBI with ECH plasma. It becomes under $1\,\mathrm{m^2/s}$ at $\rho > 0.1$ with the steep ∇T_e.

Figure 1(c) shows the power balance of electrons and ions in a NBI with ECH plasma ($\triangle$ in Fig.1(a)). The notations of p_{ECH}, p^e_{NBI}, p_{ei}, p_{rad}, p_{conv} and p_{cond} in the figure of the T_e equation represent the ECH absorbed power, the NBI heating power to electrons, electron-ion rethermalization, radiation loss, convection loss and radial transport, respectively. In the figure of the T_i equation, p^i_{NBI}, p_{ion} and p_{cx} are the NBI heating power to ions, the energy loss due to neutral ionization and the charge exchange loss, respectively. p_{ECH} is localized at the resonance position of the normalized minor radius $\rho \simeq 0.1$ and its peak value exceeds $1\,\mathrm{MW/m^3}$. On the other hand, p^e_{NBI} has a broad profile and it is usually less than $100\,\mathrm{kW/m^3}$. Especially, it is less than about $40\,\mathrm{kW/m^3}$ in this figure because of the low n_e. p^i_{NBI} is also about $40 \sim 50\,\mathrm{kW/m^3}$ near the center in this case.

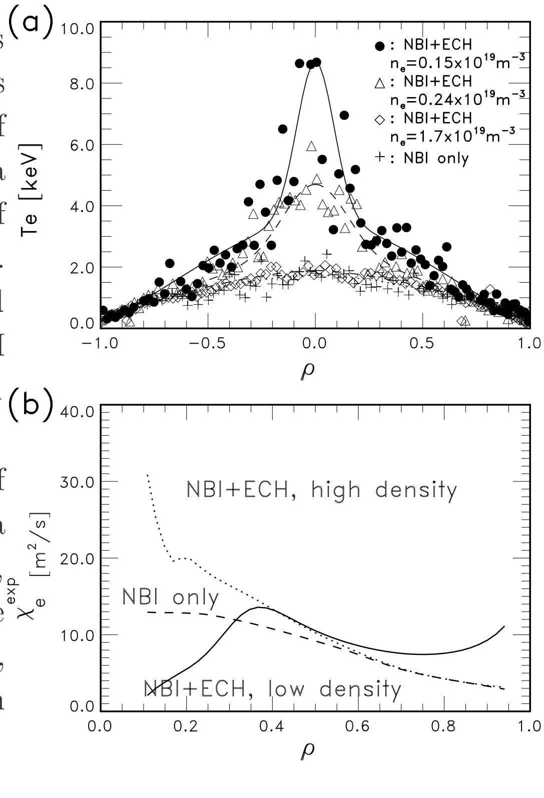

Figure 1. (a) T_e profiles of three NBI with ECH plasmas and a NBI-only plasma, (b) χ_e of high and low density NBI with ECH plasmas and a NBI-only plasma, (c) the power balance of electrons and ions in a low density NBI with ECH plasma.

Figure 2(a) shows the neoclassical E_r^{neo} which are calculated by the condition of $\Gamma_e^{asym} = \sum Z_j {\Gamma_i^{asym}}_j$ [9], where Γ_e^{asym} and Γ_i^{asym} are the asymmetric part of the neoclassical electron and ion flux, respectively. E_r^{neo} in the low density NBI with ECH plasma is positive in the whole plasma and it shows a peak at the central region. This spatial profile is similar with the experimentally observed E_r by CXS with neon gas puffing in the plasmas of $n_e > 0.5 \times 10^{19}\,\mathrm{m}^{-3}$, but the magnitude of E_r^{neo} is larger than the E_r^{CXS} by about factor of 2. On the other hand, E_r^{neo} in the NBI-only or the high density plasmas shows negative or small positive values and multiple roots of E_r appear in the NBI-only case. It may be considered that the neoclassical E_r^{neo} affects on the improvement of χ_e in the ECH overlapped plasmas. However, the neoclassical χ_e^{neo} with E_r^{neo} is smaller than χ_e^{exp} by about one order, as seen in Fig.2(b).

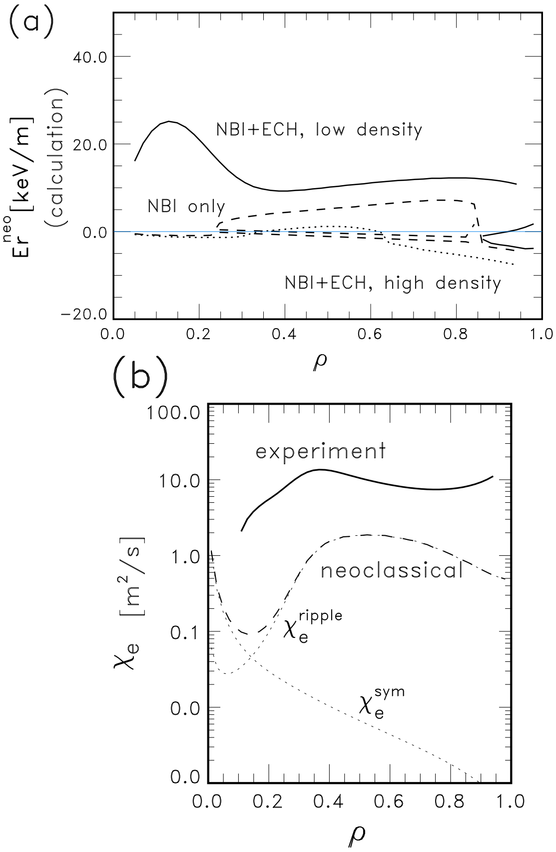

Figure 2. (a) Neoclassical E_r^{neo} in high and low density NBI with ECH plasmas and a NBI-only plasma, (b) $\chi_e^{exp} and \chi_e^{neo}$ in a low density NBI with ECH plasma.

3. Simulations of the temporal development of the electron temperatures

The transport coefficients which are derived by the steady state analysis are still ambiguous at the central region of $\rho < 0.1$ as the power absorption profile of ECH by ray-tracing method shows small value at the vicinity of $\rho = 0$. In order to evaluate χ_e near the center, the temporal development of T_e measured by ECE [10], T_e^{ECE}, are studied. Figure 3(a) shows T_e^{ECE} and the results of transport simulation at $\rho = 0.03$, 0.085 and 0.434. This calculated T_e are derived by assuming a certain χ_e after the ECH off time.

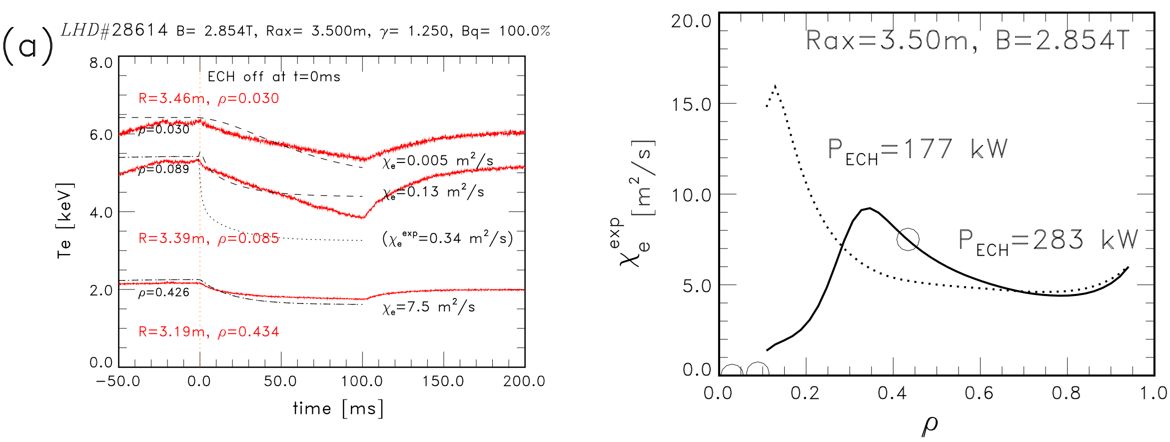

Figure 3. (a) the ECE signals and the simulated temporal development of T_e, (b) χ_e^{exp} in the NBI with ECH plasmas at $R_{ax} = 3.50\,\mathrm{m}$ and $B = 2.895\,\mathrm{T}$. The symbol, ○, denotes the values which are used in this simulation.

These ECH modulation experiments were operated under the conditions of $R_{ax} = 3.50\,\mathrm{m}$ and $B = 2.895\,\mathrm{T}$ with the ECH power of 283 kW and 177 kW. In the higher P_{ECH} case, the T_e profile has a steep gradient and the decay times, τ_d, of T_e^{ECE} are more than 100 ms at the central region, while no steep gradient was observed and $\tau_d \simeq 20\,\mathrm{ms}$ in the lower P_{ECH} case.

The simulation of T_e are carried out from an initial profile measured by the Thomson scattering and therefore, the magnitude of T_e^{ECE} are calibrated by the temperatures of Thomson scattering. The dotted curve in Fig.3(a) shows a example of the results of the calculation by using χ_e^{exp}, which is shown in Fig.3(b) (solid curve). The decay time of this case is smaller than that of the ECE results. The dashed curves in Fig.3(a) are the calculation results by using some assumed χ_e which are selected in order to reproduce the time development of T_e^{ECE}. Although these simulation results are not completely agree with the experimental data, the longer decay times of $50 \sim 100\,\mathrm{ms}$ can be reproduced.

The values of χ_e assumed in Fig.3(a) are plotted in Fig.3(b) (○). The assumed χ_e is $0.005\,\mathrm{m}^2/\mathrm{s}$ at $\rho \sim 0.03$ and $0.13\,\mathrm{m}^2/\mathrm{s}$ at $\rho \sim 0.08$. It may be considered that these small χ_e values indicate some improvement of electron thermal transport at the center.

4. Summary

The local electron thermal transport was investigated for the low density NBI with ECH plasmas on LHD. The derived χ_e^{exp} was reduced with the steep gradient of T_e near the center, but the values of χ_e^{exp} are still larger than the neoclassical χ_e^{neo}. The radial electric field predicted by the neoclassical theory, E_r^{neo}, is also calculated. Although the magnitude of E_r^{neo} is larger than the experimentally measured E_r^{CXS}, their radial profiles are similar. Some ambiguity remains in the steady state analysis of χ_e at the center. However, the electron thermal transport at the central region seems to be improved from the view point of the temporal development of T_e by comparing the ECE signals with the results of transport simulation.

References

[1] A.Iiyoshi, A.Komori, *et.al.*, Nucl.Fusion**39**(1999)1245.
[2] S.Kubo,T.Shimozuma,*et.al.*,Journal of Plasma and Fusion Research **78**(2002)99.
[3] A.Fujisawa, H.Iguchi, T.Minami *et.al.*, Phys.Rev.Lett.**29**(1999)2669.
[4] K.Narihara,*et.al.*,Rev.Sci.Instrum.**72**(2001)1122.
[5] K.Ida, S.Kado *et.al.*, Rev.Sci.Instrum.**71**(2000)2360.
[6] K.Ida, Plasma Phys.Control.Fusion**40**(1998)1429.
[7] H.C.Howe, ORNL/TM-11521(1990).
[8] S.Murakami, N.Nakajima and M.Okamoto, Trans.Fusion Technol.**27**(1995)256.
[9] M.Yokoyama, K.Ida *et.al.*,Nucl.Fusion**42**(2002)143.
[10] Y.Nagayama,*et.al.*,Rev.Sci.Instrum.**70**(1999)1021.